Vaporization Thermodynamic Studies by High-Temperature Mass Spectrometry on Some Three-Phase Regions over the $MnO-TeO_2$ Binary Line in the Mn−Te−O Ternary System

T. S. Lakshmi Narasimhan, M. Sai Baba, and R. Viswanathan*

Fuel Chemistry Division, Chemistry Group, Indira Gandhi Centre for Atomic Research, Kalpakkam, Tamil Nadu 603102, India

Received: June 27, 2006; In Final Form: October 11, 2006

Knudsen effusion mass spectrometric measurements have been performed in the temperature range of 850−950 K over four three-phase mixtures, each phase mixture having at least one phase lying on the $MnO-TeO_2$ binary line of the Mn−Te−O phase diagram, and the rest of the phases lying above this binary line. The three-phase mixtures investigated are $Mn_3O_4 + MnO + Mn_6Te_5O_{16}$; $Mn_3O_4 + Mn_6Te_5O_{16} + MnTeO_3$; $Mn_3O_4 + Mn_3TeO_6 + MnTeO_3$; and $Mn_3TeO_6 + MnTeO_3 + Mn_2Te_3O_8$. The vapor pressures of the gaseous species TeO_2, TeO, and Te_2 over these three-phase mixtures were measured, and various heterogeneous solid−gas reactions were evaluated along with the homogeneous gas-phase reaction $TeO_2(g) + 0.5Te_2(g) = 2\,TeO(g)$. The enthalpy and Gibbs free energy of formation of the four ternary Mn−Te−O phases were deduced at $T = 900$ K. These values (in kJ·mol^{-1}), along with the estimated uncertainties in them are $\Delta_f H^o_m = 4150 \pm 19$, 752 ± 11, 1710 ± 11, 1924 ± 40, and $\Delta_f G^o_m = 2835 \pm 28$, 511 ± 11, 1254 ± 19, 1238 ± 38, for $Mn_6Te_5O_{16}$, $MnTeO_3$, Mn_3TeO_6, and $Mn_2Te_3O_8$, respectively. A thermochemical assessment was made to examine the conditions under which the ternary Mn−Te−O phases could be formed on a stainless steel clad of mixed-oxide-fuelled (MO_2; M = U + Pu) fast breeder nuclear reactors. The phase Mn_3TeO_6 could be formed when the fuel is even slightly hyperstoichiometric (O/M = 2.0002) and the phase $Mn_6Te_5O_{16}$ could also be formed when O/M = 2.0004. The threshold tellurium potential for the formation of Mn_3TeO_6 is higher than that for $MnTe_{0.80}$ and $CrTe_{1.10}$, but is comparable to that for $MoTe_{1.10}$, and even lower than that for $FeTe_{0.81}$ or $NiTe_{0.63}$.

Introduction

Having established the ternary phase diagram of the Mn−Te−O system at 950 K in the composition range in and around the $MnO-TeO_2$ pseudo-binary line,[1] and having performed a number of isothermal vaporization experiments that confirmed the existence of a quasi-congruently vaporizing three-phase equilibrium ($MnTeO_3 + Mn_3TeO_6 +$ vapor)[2] in the Mn−Te−O system, we continued to investigate this system further. We have conducted systematic vaporization studies over the four three-phase regions $Mn_3O_4 + MnO + Mn_6Te_5O_{16}$; $Mn_3O_4 + Mn_6Te_5O_{16} + MnTeO_3$; $Mn_3O_4 + Mn_3TeO_6 + MnTeO_3$; and $Mn_3TeO_6 + MnTeO_3 + Mn_2Te_3O_8$ in the temperature range 850−950 K. The main objectives were to obtain $p-T$ relations for the gaseous species $TeO_2(g)$, TeO(g), and $Te_2(g)$ in the equilibrium vapor over these phase fields, deduce thermodynamic data for various heterogeneous reactions in each phase field as well as for the homogeneous gas-phase reaction $TeO_2(g) + 0.5Te_2(g) = 2TeO(g)$, and finally deduce the thermodynamic data for the ternary phases $Mn_6Te_5O_{16}$, $MnTeO_3$, Mn_3TeO_6, and $Mn_2Te_3O_8$. To our knowledge, the only thermodynamic data available in the literature are the heat capacities for the phases $MnTeO_3$, $Mn_2Te_3O_8$, and $MnTe_2O_5$ reported by Gospodinov and Mihov.[3] Our interest in vaporization thermodynamic studies of the Mn−Te−O system was basically motivated by our belief that, for a better understanding of fission-product tellurium-assisted clad corrosion in mixed-oxide-fuelled fast breeder nuclear reactors, one needs to consider the formation of ternary oxide phases involving tellurium and stainless steel (SS) clad components in addition to that of binary tellurides. Especially so, if the O/M (M = U + Pu) of the fuel outer-surface were to ever become hyper-stoichiometric, that is, greater than 2. Accordingly, in addition to basic thermodynamic data such as vapor pressures, enthalpy, and Gibbs free energy change for various reactions, we report in this paper an estimate of the threshold tellurium potential required for the formation of ternary Mn−Te−O phases on an SS clad of mixed-oxide-fuelled fast breeder reactors and compare them with those that could exist in the fuel−clad gap. Since our investigations on binary metal tellurides led us to infer that the lowest tellurium activity is required for the formation of manganese telluride,[4,5] we began the ternary systems investigations with that on the Mn−Te−O system.

Experimental

Sample Preparation. The starting materials used for the preparation of different samples were MnO(s) (Aldrich Chemical Co., Inc.; purity: 99.99%), TeO_2(s) (Leico Industries, Inc.; purity: 99.99%), $MnCO_3$(s) (Aldrich Chemical Co., Inc.; purity: 99.9%) and Mn(s) (Leico Industries, Inc.; purity: 99.9%). Thoroughly ground and homogenized mixtures of the starting materials were made into pellets of 10 mm diameter and placed in a platinum crucible or boat and heated. The preparation of the samples pertinent to this paper involved the use of two methods: the "vacuum-seal" method (or static method), and the "flowing-argon" method (or dynamic method). In the vacuum-seal method, the pellets were placed in a platinum

* To whom correspondence should be addressed. Fax: 91 44 27480065; e-mail: rvis@igcar.gov.in.

10.1021/jp064011b CCC: $33.50
Published on Web 12/02/2006

TABLE 1: Sample Preparation Details

sample no.[a]	starting materials	preparation method	effective starting composition	phase field[b]
BS#8	Mn, MnO, TeO_2	flowing- argon	$Mn_{0.35}Te_{0.16}O_{0.49}$	3P1: $Mn_3O_4 + MnO + Mn_6Te_5O_{16}$
BS#9	Mn, MnO, TeO_2	flowing- argon	$Mn_{0.34}Te_{0.17}O_{0.49}$	3P1: $Mn_3O_4 + MnO + Mn_6Te_5O_{16}$
BS#10	Mn, MnO, TeO_2	flowing- argon	$Mn_{0.35}Te_{0.16}O_{0.49}$	3P1: $Mn_3O_4 + MnO + Mn_6Te_5O_{16}$
BS#11	Mn, MnO, Mn_3TeO_6[c]	vacuum-seal	$Mn_{0.39}Te_{0.06}O_{0.55}$	3P1: $Mn_3O_4 + MnO + Mn_6Te_5O_{16}$
BS#12	MnO, TeO_2	vacuum-seal	$Mn_{0.36}Te_{0.10}O_{0.54}$	3P2: $Mn_3O_4 + Mn_6Te_5O_{16} + MnTeO_3$
BS#13	$MnCO_3$, TeO_2	flowing- argon	$Mn_{0.36}Te_{0.10}O_{0.54}$	3P3: $Mn_3O_4 + Mn_3TeO_6 + MnTeO_3$
BS#14	$MnCO_3$, TeO_2	flowing- argon	$Mn_{0.20}Te_{0.20}O_{0.60}$	3P4: $Mn_3TeO_6 + MnTeO_3 + Mn_2Te_3O_8$
BS#17	$MnCO_3$, TeO_2	flowing- argon	$Mn_{0.17}Te_{0.22}O_{0.61}$	3P4: $Mn_3TeO_6 + MnTeO_3 + Mn_2Te_3O_8$

[a] BS designates bulk-sample. [b] Three-phase fields designated as 3P1, 3P2, 3P3, and 3P4. [c] Pellets of composition ($3MnO + 1TeO_2$) placed in a platinum boat and heated inside the mullite tube of a horizontal furnace at 950 K for ~25 h in open air.

boat and inserted into a quartz tube (length: 80−100 mm; diameter: 15 mm), which was alternately evacuated and flushed with argon several times before being sealed under a residual pressure of $\sim 10^{-4}$ Pa. The pellets were heated at 875 K for 24 h and at 950 K for 60 h. In the flowing-argon method, the pellets were placed in a platinum boat and inserted into a long horizontal quartz tube (length: 70 cm; diameter: 35 mm), the inlet of which was connected to an argon gas cylinder through a dehydrating medium, and the outlet was set in water kept inside a beaker. The pellets were heated in a dynamic mode under flowing argon at 875 K for 8−10 h and at 950 K for 15−20 h. Table 1 gives the details of the samples prepared. More details on the sample preparation and reasons for the use of different methods of preparation are given in refs 1, 2, and 6.

Mass Spectrometric Studies. A VG Micromass mass spectrometer (MM 30 BK) was employed for the vaporization studies. Three aliquots were used from each of the bulk samples BS#9, BS#12, BS#13, and BS#17. With the first aliquot, an isothermal experiment at 950 K was performed, while, with each of the other two aliquots, one or a maximum of two temperature dependence runs in the range 850−950 K were performed. Vaporization was effected from an alumina Knudsen cell (i.d.: 7.5 mm; o.d.: 10.0 mm; height: 10.0 mm; orifice (knife edged) diameter: 0.5 mm) having a platinum liner. The alumina Knudsen cell was placed inside a molybdenum cup having a removable but tightly fitting lid made of tungsten with a 3 mm diameter hole collinear with the Knudsen-cell orifice. This assembly was heated by means of electron bombardment from two encircling tungsten filaments. Temperatures were measured by a chromel-to-alumel thermocouple, inserted through the base of the molybdenum cup (so as to always touch the base of the alumina Knudsen cell) and calibrated against the melting temperature of silver. With excellent temperature control, permitted by the "thermocouple control mode" of heating, the temperature measurement was accurate within ±3 K.

The mass spectra of the equilibrium vapor over all the samples consisted of peaks due to Te^+, Te_2^+, TeO^+, TeO_2^+, and O_2^+. The neutral species were ascertained to be $Te_2(g)$, TeO(g), TeO_2-(g), and $O_2(g)$. As over $TeO_2(s)$,[7] the ion Te^+ was found to be a fragment ion having its origin mainly from TeO(g). Because of the high background at the mass where the ion O_2^+ was detected, the ion intensities of O_2^+ were measured only occasionally, considered unreliable, and not used in any evaluation.

In each isothermal experiment, the intensities of $^{130}Te^+$, ^{256}-Te_2^+, $^{146}TeO^+$, and $^{162}TeO_2^+$ ions were measured as a function of time at 950 K at an electron energy of 37.3 eV. The experiment was terminated when the intensities remained constant for a sufficiently long time (a minimum of ~4 h) to be eligible for ascription to an univariant vaporization equilibrium. Each temperature-dependence experiment was conducted such that (1) the intensities of $^{130}Te^+$, $^{256}Te_2^+$, $^{146}TeO^+$, and $^{162}TeO_2^+$ ions were measured at 37.3 eV at all temperatures and additionally at 13.0 eV at 950 K, (2) the second run, whenever conducted, was a continuation of the first run in the opposite temperature direction, and (3) the total duration at the highest temperature of 950 K inclusive of both runs was never more than 3 h. The residue from every experiment was subjected to X-ray diffraction investigation to confirm that it contained all the phases that were originally present and had no new phase.

Pressure calibration experiments were performed by taking solid TeO_2 in the same Knudsen cell used for Mn−Te−O samples. After each pressure calibration experiment, the Knudsen cell was thoroughly degassed at $T \approx 1300$ K so that the ion intensities of Te or Te + O ionic species at $T = 950$ K were not detectable or insignificant. More details on the mass spectrometric measurements are given elsewhere.[1,2,6]

Results and Discussion

Comparison of the ionization efficiency curves obtained over Mn−Te−O samples with those over TeO_2[7] confirmed that Te^+ was a fragment ion, mainly of TeO(g), and that, at 13 eV, fragmentation is minimized for all species. Figure 1 shows the pertinent portions of the ionization efficiency curves of Te^+, Te_2^+, TeO^+, and TeO_2^+ obtained over $MnO + Mn_3O_4 + Mn_6Te_5O_{16}$.

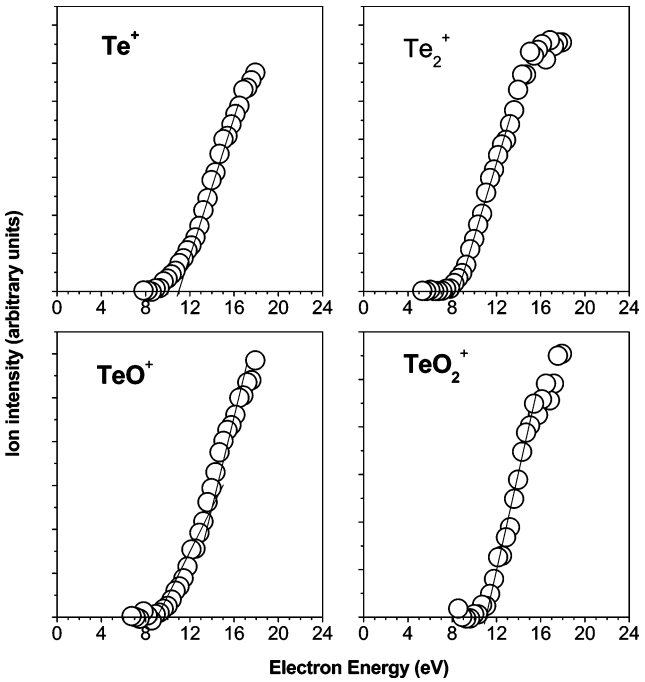

Figure 1. Pertinent portions of the ionization efficiency curves for Te^+, Te_2^+, TeO^+, and TeO_2^+ obtained over 3P1 ($MnO + Mn_3O_4 + Mn_6Te_5O_{16}$).

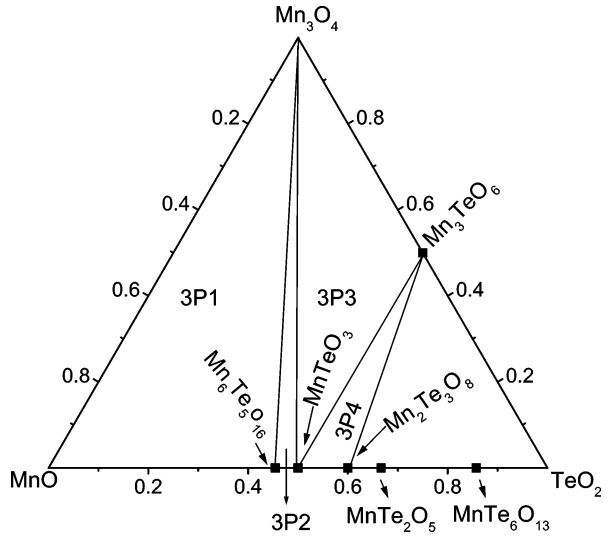

Figure 2. An expanded version of the phase diagram of the ternary Mn−Te−O system at $T = 950$ K.[1]

The measured ion intensities I at temperature T were converted to partial pressures p by using the following equations:

$$p(i,T) = k'(i)I(i^+,13.0\text{ eV},T)T \quad (1)$$

$$k'(i) = k'(j)\{\sigma(j)/\sigma(i)\}\{\gamma(j^+)/\gamma(i^+)\}\{n(j^+)/n(i^+)\} \text{ where } j = \text{TeO}_2 \text{ and } i = \text{TeO}_2, \text{Te}_2, \text{ and TeO} \quad (2)$$

$$I(i^+,13.0\text{ eV},T) = \{I(i^+,37.3\text{ eV},T)/F(i^+)\} \quad (3)$$

$$F(i^+) = I(i^+,37.3\text{ eV},950\text{ K})/I(i^+,13.0\text{ eV},950\text{ K}) \quad (4)$$

In the case of TeO^+, the ion intensity of Te^+ was added to that of TeO^+ by assuming that, even at 13.0 eV, the entire $I(Te^+)$ was due to the dissociative ionization of TeO(g):

$$I(i^+,13.0\text{ eV},T) = \{I(i^+,37.3\text{ eV},T)/F(i^+)\} + \{I(j^+,37.3\text{ eV},T)/F(j^+)\}\{\gamma(i^+)/\gamma(j^+)\}\{n(i^+)/n(j^+)\} \text{ where } i = \text{TeO and } j = \text{Te} \quad (5)$$

In above equations, k' and σ denote the pressure calibration constant and the relative ionization cross-section of the gaseous species, respectively; γ and n denote the relative detector response and the relative isotope abundance of the ionic species, respectively. The primary pressure calibration constant $k'(TeO_2)$ was obtained from $I(TeO_2^+,13.0\text{ eV})$ measured over $TeO_2(s)$ and by using a known $p(TeO_2)$ over $TeO_2(s)$[7] and eq 1. The relative detector response γ is the ratio of ion intensities at $T = 950$ K measured with the secondary electron multiplier to that measured with a Faraday cup.

Tables 1S−4S (Supporting Information) give the ion intensities measured at 37.3 eV over different three-phase fields. The tables also contain the values of all other parameters that have been employed to obtain partial pressures according to eqs 1−5. The relative ionization cross-sections at 13.0 eV for $\sigma(Te_xO_y)$ were computed by using the empirical relation $\sigma(Te_xO_y) = 0.75\text{-}[x\sigma(Te) + y\sigma(O)]$[8] and from the values given by Mann[9] for elements. The σ values used were 4.46×10^{-16} cm^2 for Te_2; 2.23×10^{-16} cm^2 for TeO; and 2.23×10^{-16} cm^2 for TeO_2.

For clarity, we designated the three-phase fields investigated in this work as 3P1, 3P2, 3P3, and 3P4 (see Table 1), all having at least one phase that lies on (and the rest of the phases lie above) the MnO−TeO_2 binary line of the ternary phase diagram Mn−Te−O.[1] Figure 2 shows an expanded version of the phase diagram of the ternary Mn−Te−O system at $T = 950$ K.

The designation is made such that 3P1 refers to the three-phase field on the left-most part of the phase diagram, and 3P2, 3P3, and 3P4 refer to those that lie successively adjacent: 3P1 is composed of two binary phases, Mn_3O_4 and MnO, and a ternary phase, $Mn_6Te_5O_{16}$, the most MnO-rich phase on the MnO−TeO_2 binary line (6:5); 3P2 has a common boundary with 3P1 (Mn_3O_4−$Mn_6Te_5O_{16}$ line) and a ternary third phase $MnTeO_3$ on the MnO−TeO_2 binary line (1:1); 3P3 has a common boundary with 3P2 (Mn_3O_4−$MnTeO_3$ line) and a ternary third phase Mn_3TeO_6, which is at the intersection of the Mn_3O_4−TeO_2 (1:1) and MnO−TeO_3 (3:1) binary lines; and finally 3P4 has a common boundary with 3P3 (Mn_3TeO_6−$MnTeO_3$ line) and a ternary third phase $Mn_2Te_3O_8$ on the MnO−TeO_2 binary line (2:3).

Table 2 gives the $p-T$ relations obtained by least-squares fitting of all the partial pressure data corresponding to each three-phase field. It also gives the values of the partial pressures at $T_m = 900$ K. A plot of the partial pressures against the reciprocal temperature is given in Figure 3. The uncertainty in the partial pressures could be ∼20−30%, as estimated from the uncertainties in pressure calibration and other factors used in computations. From the results given in Table 2, one infers that (1) over

TABLE 2: $p-T$ Relations in the Temperature Range $T = 850-950$ K and Partial Pressures for the Gaseous Species, Total Pressure, and Relative Compositions Neglecting the Contribution of O_2(g)

		$\log(p/\text{Pa}) = -A/T + B$			
phase field	species	A	B	p/Pa at $T = 900$ K	relative composition at $T = 900$ K ($p(i)/p$(total))
3P1: Mn_3O_4 + MnO + $Mn_6Te_5O_{16}$	TeO_2(g)	15049 ± 108	14.381 ± 0.120	4.57×10^{-3}	0.131
	TeO(g)	14965 ± 218	14.830 ± 0.241	1.59×10^{-2}	0.456
	Te_2(g)	15100 ± 190	14.938 ± 0.211	1.45×10^{-2}	0.414
	total pressure, p(total) =			3.50×10^{-2}	
3P2: Mn_3O_4 + $Mn_6Te_5O_{16}$ + $MnTeO_3$	TeO_2(g)	14037 ± 237	13.295 ± 0.263	4.99×10^{-3}	0.159
	TeO(g)	14472 ± 157	14.246 ± 0.174	1.47×10^{-2}	0.468
	Te_2(g)	15344 ± 189	15.117 ± 0.209	1.17×10^{-2}	0.373
	total pressure, p(total) =			3.13×10^{-2}	
3P3: Mn_3O_4 + $MnTeO_3$ + Mn_3TeO_6	TeO_2(g)	13881 ± 143	12.926 ± 0.159	3.18×10^{-3}	0.148
	TeO(g)	14072 ± 91	13.634 ± 0.101	9.96×10^{-3}	0.465
	Te_2(g)	14903 ± 165	14.477 ± 0.183	8.28×10^{-3}	0.386
	total pressure, p(total) =			2.14×10^{-2}	
3P4: $MnTeO_3$ + Mn_3TeO_6 + $Mn_2Te_3O_8$	TeO_2(g)	15694 ± 139	15.864 ± 0.155	2.67×10^{-2}	0.457
	TeO(g)	15378 ± 552	15.538 ± 0.612	2.83×10^{-2}	0.484
	Te_2(g)	14671 ± 671	13.836 ± 0.744	3.43×10^{-3}	0.059
	total pressure, p(total) =			5.84×10^{-2}	

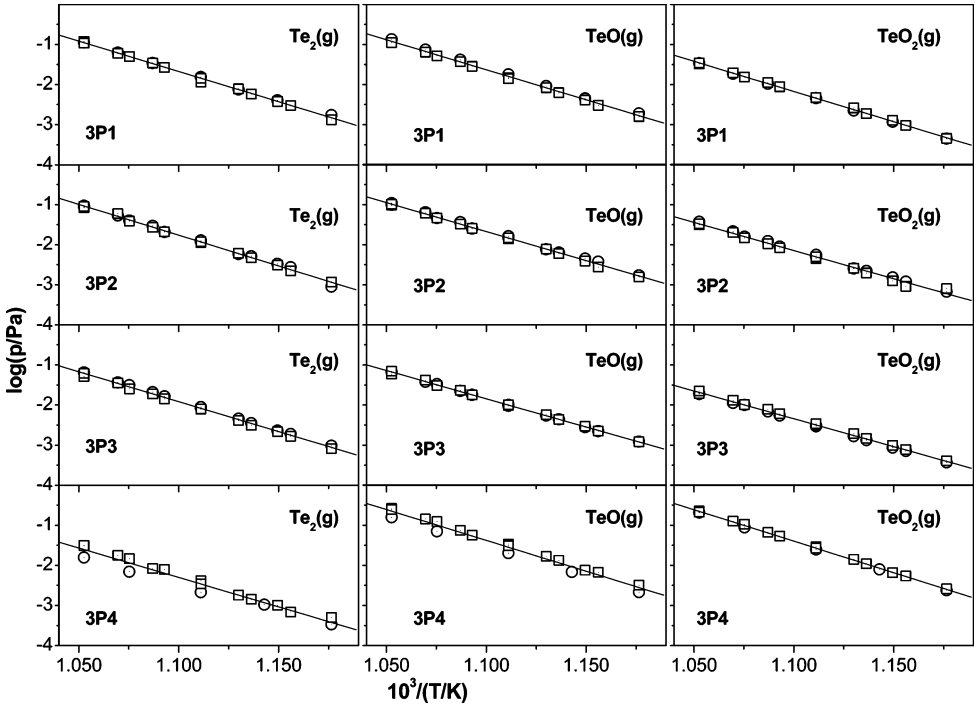

Figure 3. A plot of partial pressures against reciprocal temperature over various three-phase regions; (○) aliquot 2; (□) aliquot 3.

all of the four three-phase fields, TeO(g) is the most dominant species (45−48% of the vapor phase); (2) over 3P1, 3P2, and 3P3, TeO_2(g) constitutes only about 13−16%, whereas Te_2(g) is a close second to TeO(g); (3) over 3P4, however, TeO_2(g) is a close second to TeO(g) with Te_2 constituting only ∼6%. Comparison of the absolute values of partial pressures shows that, relative to the values corresponding to 3P1, the values for 3P2 are not very different, and the values for 3P3 are also lower only by a small percentage of about 30−40%, but the values for 3P4 are distinctly different, the $p(TeO_2)$ being higher by a factor of 6, the p(TeO) being higher by a factor of 2, and the $p(Te_2)$ being lower by a factor of 4. We are unable to assign specific reasons for such results. The only known facts are that 3P1, 3P2, and 3P3 all have Mn_3O_4 as a common phase, and 3P4 has three ternary phases.

We restricted our measurements to $T = 950$ K, although the total vapor pressure at this temperature was never greater than 0.5 Pa in any of the three-phase fields. We were guided by the information obtained by Ivanova[10] through a differential thermal analysis study of MnO−TeO_2 binary system: there exists an eutectic between $Mn_2Te_3O_8$ and $MnTeO_3$ at $T \approx 950$ K (at a composition of 55 mol % TeO_2), and $Mn_2Te_3O_8$ melts congruently at 993 K. We obtained no indication of liquid phase formation, but rather only confirmation that the vaporization residues contained the same three phases that were present initially.

With no Mn-bearing species in the vapor phase, how the overall composition of the samples will change upon vaporization from a Knudsen cell can be inferred by calculating the Te-to-O ratio in the effusate by applying the well-known effusion equation.[11,12] We performed these calculations by using the partial pressures given in Table 2 but ignoring $p(O_2)$, which we did not measure. The values that we refer to as "the apparent Te-to-O ratio in the effusate" are ∼1.6 ± 0.1 for 3P1, 3P2, and 3P3, and ∼ 0.74 for 3P4. If $p(O_2)$, which was not measured by us, were to be taken into account, the values of the Te-to-O ratio in the effusate will decrease, but the extent of decrease will be relatively much less for 3P1, 3P2, and 3P3 when compared to that for 3P4. The reason being that the $p(O_2)$ over 3P4 relative to that over the other three-phase regions would be 9−12 times too high, as can be deduced from the values of p(TeO)/$p(TeO_2)$ and $p(Te_2)/p(TeO_2)^2$ ratios, and by applying mass-action law to the gas-phase equilibria $TeO_2(g) = TeO(g) + 0.5\ O_2(g)$ and $2TeO_2(g) = Te_2(g) + 2O_2(g)$. At $T = 900$ K, for instance, the $p(TeO)/p(TeO_2) = 1.1$ and $p(Te_2)/p(TeO_2)^2 = 5$ over 3P4, whereas the mean of values over the other three-

TABLE 3: Thermodynamic Data Deduced from Partial Pressures for Various Reactions

reaction	$\Delta_r H°_m$ (900 K) (kJ•mol^{-1})	$\Delta_r S°_m$ (900 K) (J•mol^{-1}•K^{-1})	$\Delta_r G°_m$ (900 K) (kJ•mol^{-1})
3P1: (Mn_3O_4 + MnO + $Mn_6Te_5O_{16}$)			
$Mn_6Te_5O_{16}(s) + Te_2(g) = 3MnO(s) + Mn_3O_4(s) + 2TeO_2(g) + 5TeO(g)$	1719.9 ± 18.6	1109.5 ± 20.7	721.3 ± 18.6
$Mn_6Te_5O_{16}(s) = 6MnO(s) + 5TeO_2(g)$	1440.8 ± 10.4	897.8 ± 11.5	632.9 ± 10.4
3P2: (Mn_3O_4 + $Mn_6Te_5O_{16}$ + $MnTeO_3$)			
$Mn_6Te_5O_{16}(s) + TeO_2(g) + Te_2(g) = Mn_3O_4(s) + 3MnTeO_3(s) + 5TeO(g)$	823.0 ± 11.1	532.4 ± 12.3	343.8 ± 11.1
$6MnTeO_3(s) = Mn_6Te_5O_{16}(s) + TeO_2(g)$	268.8 ± 4.5	158.7 ± 5.0	125.9 ± 4.5
3P3: (Mn_3O_4 + Mn_3TeO_6 + $MnTeO_3$)			
$3Mn_3TeO_6(s) + TeO_2(g) + Te_2(g) = 2Mn_3O_4(s) + 3MnTeO_3(s) + 3TeO\ (g)$	257.2 ± 2.6	162.6 ± 2.9	110.8 ± 2.6
$Mn_3TeO_6(s) = Mn_3O_4(s) + TeO_2(g)$	265.8 ± 2.7	151.7 ± 3.0	129.3 ± 2.7
3P4: (Mn_3TeO_6 + $MnTeO_3$ + $Mn_2Te_3O_8$)			
$MnTeO_3(s) + Mn_2Te_3O_8(s) + 3TeO(g) = Mn_3TeO_6(s) + 4TeO_2(g) + Te_2(g)$	599.6 ± 13.9	395.8 ± 15.5	243.4 ± 13.9
$Mn_2Te_3O_8(s) = 2MnTeO_3(s) + TeO_2(g)$	300.5 ± 2.7	207.9 ± 3.0	113.4 ± 2.7

TABLE 4: Enthalpy and Gibbs Free Energy of Formation of Ternary Phases Deduced by the Evaluation of Various Reactions 6−13

phase	reaction employed	$\Delta_f H^\circ_m$(900 K) (kJ·mol^{-1})	$\Delta_f G^\circ_m$(900 K) (kJ·mol^{-1})
$Mn_6Te_5O_{16}$	6	4167 ± 19	2807 ± 19
	7	4134 ± 10	2863 ± 10
	recommended (mean value) =	4150 ± 19	2835 ± 28
$MnTeO_3$	8	755 ± 11	518 ± 11
	9	750 ± 5	504 ± 5
	recommended (mean value) =	752 ± 11	511 ± 11
Mn_3TeO_6	10	1698 ± 3	1235 ± 3
	11	1721 ± 3	1273 ± 3
	recommended (mean value) =	1710 ± 11	1254 ± 19
$Mn_2Te_3O_8$	12	1964 ± 14	1276 ± 14
	13	1883 ± 3	1199 ± 3
	recommended (mean value) =	1924 ± 40	1238 ± 38

phase regions are 3.2 ± 0.3 for $p(TeO)/p(TeO_2)$ and 660 ± 160 for $p(Te_2)/p(TeO_2)^2$. Comparison with the results over TeO_2(s), which is known to vaporize congruently, will be of interest: $p(TeO)/p(TeO_2) = 0.62$ and $p(Te_2)/p(TeO_2)^2 = 0.35$; the Te-to-O ratio in the effusate is 0.50 (applying congruent vaporization conditions) and the apparent Te-to-O ratio in the effusate is ∼0.7 (ignoring $p(O_2)$). Although $p(O_2)$ over 3P4 relative to that over TeO_2(s) would be about 3 times too low, we take all this information to indicate that the vaporization of 3P4 from a Knudsen cell will result in a change of composition mainly corresponding to a loss of TeO_2 units, whereas the vaporization of 3P1, 3P2, and 3P3 will result in a relatively greater loss of tellurium. Reference to TeO_2 units is made here specially because all four three-phase regions that have been investigated in this work have at least one phase that can be assigned on the MnO−TeO_2 binary line and the other (phase or) phases lying above (the O-rich side of) this binary line.

From the partial pressures, the Gibbs free energy changes were deduced for two types of reactions in each three-phase region: one which involves participation by all three condensed phases and all three gaseous species, whose partial pressures were measured; and another which involves the decomposition of a ternary condensed phase to a binary (Mn + O) phase or another ternary phase through the loss of TeO_2(g). The enthalpy and entropy changes for these reactions at $T = 900$ K were also deduced by the "second law method".[11]

Three-phase region 3P1:

$$Mn_6Te_5O_{16}(s) + Te_2(g) = 3MnO(s) + Mn_3O_4(s) + 2TeO_2(g) + 5TeO(g) \quad (6)$$

$$Mn_6Te_5O_{16}(s) = 6MnO(s) + 5TeO_2(g) \quad (7)$$

Three-phase region 3P2:

$$Mn_6Te_5O_{16}(s) + TeO_2(g) + Te_2(g) = Mn_3O_4(s) + 3MnTeO_3(s) + 5TeO(g) \quad (8)$$

$$6MnTeO_3(s) = Mn_6Te_5O_{16}(s) + TeO_2(g) \quad (9)$$

Three-phase region 3P3:

$$3Mn_3TeO_6(s) + TeO_2(g) + Te_2(g) = 2Mn_3O_4(s) + 3MnTeO_3(s) + 3TeO(g) \quad (10)$$

$$Mn_3TeO_6(s) = Mn_3O_4(s) + TeO_2(g) \quad (11)$$

Three-phase region 3P4:

$$Mn_2Te_3O_8(s) = 2MnTeO_3(s) + TeO_2(g) \quad (13)$$

$$MnTeO_3(s) + Mn_2Te_3O_8(s) + 3TeO(g) = Mn_3TeO_6(s) + 4TeO_2(g) + Te_2(g) \quad (12)$$

Results are given in Table 3. The uncertainties in the enthalpy and entropy values were deduced from standard deviations of the coefficients in $\ln K^\circ - T$ relations, where K° is the equilibrium constant computed from the partial pressures. The uncertainties in enthalpies were retained for Gibbs free energies also, despite the fact that, with the latter being deducible directly from partial pressures, the uncertainties in them could really be less than those in the enthalpies. For reaction 13, a third-law evaluation[11] was also performed. The auxiliary thermal functions required for TeO_2(g) were taken directly from the literature,[13] and, for $Mn_2Te_3O_8$(s) and $MnTeO_3$(s), they were obtained by extrapolating the reported $C_p - T$ equations[3] up to 700 K to the temperature range of the present investigation. The obtained value of third-law enthalpy at 298.15 K (290.5 ± 0.2 kJ·mol^{-1}) compared reasonably well with the second-law value (307.0 ± 2.7 kJ·mol^{-1}) considering the necessity of deducing auxiliary thermal functions by extrapolation.

The enthalpy and Gibbs free energy of formation of the ternary phases were deduced from the enthalpy and Gibbs free energy changes corresponding to reactions 6−13. The values for $Mn_6Te_5O_{16}$ at 900 K were first computed from the enthalpy and Gibbs free energies of reaction 6 as well as reaction 7 by combining them with known pertinent thermodynamic data for MnO(s),[15] Mn_3O_4(s),[15] TeO_2(g),[14] TeO(g),[14] and Te_2(g).[16] The mean value of the enthalpy or Gibbs free energy of formation corresponding to reactions 6 and 7 was then chosen as the recommended value for $Mn_6Te_5O_{16}$. Subsequently, by a similar approach, values of enthalpy and Gibbs free energy of formation for $MnTeO_3$, Mn_3TeO_6, and $Mn_2Te_3O_8$ were deduced (in succession) by using known thermodynamic data for all other participants. The results are given in Table 4. The uncertainties quoted for $\Delta_r H^\circ_m$(900 K) and $\Delta_r G^\circ_m$(900 K) in Table 3 were retained for the corresponding values of $\Delta_f H^\circ_m$ (900 K) and $\Delta_f G^\circ_m$(900 K) in Table 4. Considering the auxiliary thermodynamic information required to compute the values of enthalpy or Gibbs free energy of formation, the results deduced from the evaluation of two types of reactions are reasonably consistent: to within 1−4% for the enthalpy of formation, and within 2−6% for the Gibbs free energy of formation. The uncertainties in the recommended values of $\Delta_f H^\circ_m$(900 K) and $\Delta_f G^\circ_m$(900 K) were conservatively chosen to be the higher of either the deviation of two individual values from the mean or the maximum uncertainty in the individual values.

The following homogeneous gas-phase reaction, common to all four three-phase regions, was evaluated by second- and third-law methods:

TABLE 5: Evaluation of the Homogeneous Reaction $TeO_2(g) + 0.5Te_2(g) = 2TeO(g)$

	$\log(K^\circ) = -A/T + B$			second-law		third-law
phase region	A	B	K° at 900 K	$\Delta_r H^\circ_m$ (900 K) (kJ·mol^{-1})	$\Delta_r H^\circ_m$ (298.15 K) (kJ·mol^{-1})	$\Delta_r H^\circ_m$(298.15 K) (kJ·mol^{-1})
3P1	7331 ± 435	5.308 ± 0.483	1.45×10^{-3}	140.4 ± 8.3	141.9 ± 8.3	117.4 ± 0.4
3P2	7236 ± 224	5.136 ± 0.248	1.25×10^{-3}	138.6 ± 4.3	139.9 ± 4.3	118.6 ± 0.2
3P3	6810 ± 83	4.601 ± 0.092	1.08×10^{-3}	130.4 ± 1.6	131.8 ± 1.6	119.7 ± 0.1
3P4	7726 ± 719	5.790 ± 0.798	1.61×10^{-3}	147.9 ± 13.8	149.3 ± 13.8	116.7 ± 0.6
combined	7221 ± 257	5.138 ± 0.285	1.30×10^{-3}	138.3 ± 4.9	139.8 ± 4.9	118.3 ± 0.2
TeO_2(s)	6770 ± 150	4.825 ± 0.176	2.01×10^{-3}	129.6 ± 4.2	131.1 ± 4.2	116.2 ± 0.4

TABLE 6. Oxygen Potentials and Tellurium Potentials in the Fuel−Clad Gap Corresponding to MOX Fuels with Different O/M Ratios and Pu Fractions, and Threshold Tellurium Potentials Required for the Formation of Ternary Mn−Te−O Phases[a]

			$\Delta\mu_2$(Te) /k J·mol^{-1} for formation of $Mn_zTe_xO_y$ on SS clad			
O/M ratio in $MO_2\pm_p$	$\Delta\mu$ (O_2) (k J·mol^{-1})[b]	$\Delta\mu_1$(Te) (k J·mol^{-1}) in fuel−clad gap[c]	$Mn_6Te_5O_{16}$	$MnTeO_3$	Mn_3TeO_6	$Mn_2Te_3O_8$
		$M = U_{(1-q)}Pu_q$ (q = Pu fraction = 0.20)				
1.9998	−601	−258	442	430	222	584
2.0000	−463	−120	220	222	84	307
2.0002	−336	7	17	32	−43	54
2.0004	−326	18	1	17	−53	33
		$M = U_{(1-q)}Pu_q$ (q = Pu fraction = 0.25)				
1.9998	−595	−251	431	420	215	571
2.0000	−460	−117	216	218	81	302
2.0002	−332	11	11	26	−47	46
2.0004	−322	22	−5	11	−57	25
		$M = U_{(1-q)}Pu_q$ (q = Pu fraction = 0.30)				
1.9998	−589	−246	422	412	210	560
2.0000	−457	−114	211	214	78	296
2.0002	−328	15	5	20	−51	38
2.0004	−318	26	−12	5	−61	17

[a] T = 900 K; a(Mn) in SS = 0.0075 [b] Computed using the model reported by Krishnaiah and Sriramamurti.[19] [c] Computed by evaluating the equilibrium $Cs_2Te(s,l) + MO_2\pm_p(s) + (2 \mp p)/2O_2(g) = Cs_2MO_4(s) + Te(l)$, where ($M = U_{1-q}Pu_q$).[17]

$$TeO_2(g) + 0.5\,Te_2(g) = 2\,TeO(g) \qquad (14)$$

The necessary auxiliary thermal functions for TeO_2(g),[13] TeO(g),[13] and Te_2(g)[16] were taken from the literature. Table 5 gives the results. The partial pressures determined in various runs were all utilized to obtain a equilibrium constant−temperature relation corresponding to each three-phase region. The values of the equilibrium constant, K°, at mean T = 900 K for different three-phase regions agree well with each other and so are third-law values at T = 298.15 K. They are also in reasonable accord with the results obtained over TeO_2(s). However, the second-law values are not only uniformly higher but are also not very consistent with each other. Because the temperature range of our investigation was only 100 K and because second-law evaluation is subject to greater errors due to errors in pressure calibration between the runs, we consider the mean third-law value as more reliable.

While the present study served to obtain basic thermodynamic information on the formation of four ternary phases in the Mn−Te−O system for the first time, it also served to help us deduce information that is of relevance to nuclear technology. Since, in mixed-oxide-fuelled fast breeder nuclear reactors ($MO_2\pm_p$ where $M = U_{(1-q)}Pu_q$), an important role is attributed to tellurium in the attack of SS cladding,[17,18] thermodynamic information on compounds of tellurium with SS components are of interest to have a better understanding of the clad corrosion. Furthermore, with the oxygen potential of the fuel being a key parameter in promoting and assisting the chemical attack by an aggressive fission product such as tellurium, thermodynamic information on ternary phases formed by SS components with tellurium and oxygen also become as important as that on binary telluride phases, especially in the case of an hyperstoichiometric fuel, even if the hyperstoichiometry were to be as small as 0.0002 (i.e., p in MO_{2+p} = 0.0002). By employing the Gibbs free energy of formation of $Mn_zTe_xO_y$ determined in this work and the oxygen potentials $\Delta\mu(O_2) = RT \ln p(O_2)$ for $MO_2\pm_p$[19] as well as the activities of the SS components, a(M),[20] from the literature, the tellurium potential ($RT \ln a$(Te)), $\Delta\mu_2$(Te), required for the formation of $Mn_zTe_xO_y$ on an SS clad can be deduced by using the following relation:

$$\Delta\mu_2(\mathrm{Te}) = [\Delta_f G^\circ(Mn_zTe_xO_y) - zRT \ln a(\mathrm{Mn}) - (y/2)\Delta\mu(O_2)]/x \qquad (15)$$

Table 6 gives the results along with the values of tellurium potentials that are likely to be available in the fuel−clad gap, $\Delta\mu_1$(Te), in the case of MOX fuels ($MO_2\pm_p$; $M = U_{(1-q)}Pu_q$) corresponding to three Pu fractions (q = 0.20, 0.25, and 0.30) and for four O/M ratios (1.9998, 2.0000, 2.0002, 2.0004). If $\Delta\mu_2$(Te) < $\Delta\mu_1$(Te), there exists a possibility that the ternary Mn−Te−O phase might well be formed on an SS clad. Positive values of tellurium potentials are also listed in Table 6 (despite being meaningless) only to enable comparisons. Table 6 shows that among the four ternary phases considered, threshold tellurium potential values are the least for Mn_3TeO_6 and the greatest for $Mn_2Te_3O_8$. The values for $Mn_6Te_5O_{16}$ are less than those for $MnTeO_3$ when O/M ≥ 2 and vice versa when O/M < 2. Negative $\Delta\mu_2$(Te) values exist only for Mn_3TeO_6 (at all three Pu fractions and at O/M = 2.0002 and 2.0004) and for $Mn_6Te_5O_{16}$ (at Pu fraction = 0.30 and 0.25 and O/M = 2.0004). The values of threshold tellurium potentials (in kJ·mol^{-1}) for the formation of binary tellurides at T = 900 K are −27

($FeTe_{0.81}$), −68 ($CrTe_{1.03}$), −33 ($NiTe_{0.63}$), −50 ($MoTe_{1.10}$), and −93 ($MnTe_{0.80}$). The values for Mn_3TeO_6 at O/M = 2.0004 are more negative than those for tellurides of Fe, Ni, and Mo. Since it is known that the O/M as well as the oxygen potential of a MOX fuel increases with burn-up and that the oxygen potential would continue to increase even when the rate of increase in O/M decreases drastically after a burn-up of 6 atom % fissions,[21] we believe that the probability of the formation of ternary phases Mn_3TeO_6 and $Mn_6Te_5O_{16}$ on an SS clad clearly exists.

Conclusions

Pursuing our investigation of the Mn−Te−O system,[1,2] systematic vaporization studies were conducted on four three-phase regions, and vapor pressures and thermodynamic data for various heterogeneous reactions were obtained for the first time. Evaluation of the homogeneous gas-phase reaction $TeO_2(g) + 0.5\ Te_2(g) = 2\ TeO(g)$ provided the means of checking the consistency of measured partial pressures over the three-phase regions with those previously measured by us over congruently vaporizing $TeO_2(s)$. The results obtained in the present study led to a prediction based on a thermochemical assessment that when oxygen potentials in the fuel−clad gap of mixed-oxide-fuelled fast breeder nuclear reactors reach certain high values (as when the fuel outer surface is even slightly hyperstoichiometric or when the fuel is taken to high burn-up), ternary Mn−Te−O phases could be formed on an SS clad besides binary metal tellurides.

Acknowledgment. We dedicate this paper in memory of Prof. Klaus Hilpert (8 October 1940 to 30 September 2006) in association with whom we learned a lot on high-temperature chemistry.

Supporting Information Available: Tables 1S−4S (4 pages) give the ion intensities of Te^+, Te_2^+, TeO^+, and TeO_2^+ measured at different temperatures at an electron energy of 37.3 eV over various three-phase regions. They also give values of $F(i^+)$, $\gamma(i^+)$, $k'(i)$. This material is available free of charge via the Internet at http://pubs.acs.org.

References and Notes

(1) Lakshmi Narasimhan, T. S.; Sai Baba, M; Nalini, S; Viswanathan, R. *Thermochim. Acta* **2004**, *410*, 149.

(2) Lakshmi Narasimhan, T. S.; Sai Baba, M; Viswanathan, R. *J. Phys. Chem. B* **2002**, *106*, 6762.

(3) Gospodinov, G. G.; Mihov, D. I. *J. Chem. Thermodyn.* **1993**, *25*, 1249.

(4) Sai Baba, M.; Lakshmi Narasimhan, T. S.; Balasubramanian, R.; Mathews, C. K. *J. Nucl. Mater.* **1993**, *201*, 147.

(5) Sai Baba, M.; Viswanathan, R.; Mathews, C. K. *Rapid Commun. Mass Spectrom.* **1996**, *10*, 691.

(6) Lakshmi Narasimhan, T. S. Ph.D. Thesis, University of Madras, 2000. (e-mail: tslak@igcar.gov.in).

(7) Lakshmi Narasimhan, T. S.; Sai Baba, M.; Viswanathan, R. *Thermochim. Acta* **2005**, *427*, 137.

(8) Hilpert, K. *Structure and Bonding 73;* Springer-Verlag: Berlin, 1990; p 97.

(9) Mann, J. B. In *Recent Developments in Mass Spectrometry*, Proceedings of the International Conference on Mass Spectrometry; Ogata, K., Hayakawa, T., Eds.; University of Tokyo Press: Japan, 1970; p 814 (ionization cross-section tables obtained upon request).

(10) Ivanova, Y. Y. *Mater. Chem.* **1982**, *7*, 449.

(11) Drowart, J. In *Mass Spectrometry*, Proceedings of the International School of Mass Spectrometry; Marsel, J., Ed.; Stefan Institute: Ljubljana, Slovenia, 1971; p 187.

(12) Edwards, J. G.; Franzen, H. F. *J. Phys. Chem.* **1995**, 99, 4779.

(13) Knacke, O.; Kubaschewski, O.; Hesselmann, K. *Thermochemical Properties of Inorganic Substances*, 2nd ed.; Springer-Verlag: Berlin, 1991.

(14) Cordfunke, E. H. P.; Konings, R. J. M. *Thermochemical Data for Reactor Materials and Fission Products*; North Holland: Amsterdam, 1990.

(15) IVTANTHERMO − *A Thermodynamic Data Base and Software System for the Personal Computer*; Yungman, V. S., Medevdev, V. A., Veits, I. V., Bergman, G. A., Eds.; CRC Press and Begell House: Boca Raton, FL, 1993.

(16) Grønvold, F.; Drowart, J.; Westrum, E. F., Jr. *The Chemical Thermodynamics of Actinide Elements and Compounds. The Actinide Chalcogenides (Excluding Oxides)*; IAEA: Vienna, Austria, 1984; Part 4.

(17) Adamson, M. G.; Aitken, E. A.; Lindemer, T. B. *J. Nucl. Mater.* **1985**, *130*, 375.

(18) Adamson, M. G.; Aitken, E. A. *J. Nucl. Mater.* **1985**, *132*, 160.

(19) Krishnaiah, M. V.; Sriramamurti, P. *J. Am. Ceram. Soc.* **1984**, *67*, 568.

(20) Azad, A. M.; Sreedharan, O. M.; Gnanamoorthy, J. B. *J. Nucl. Mater.* **1987**, *144*, 94.

(21) Johnson, C. E.; Johnson, I.; Blackburn, P. E.; Crouthamel, C. E. *React. Technol.* **1972**, *15*, 303.